



ELSEVIER

Available online at www.sciencedirect.com

SCIENCE @ DIRECT®

Journal of Magnetism and Magnetic Materials 300 (2006) 53–56



www.elsevier.com/locate/jmmm

Generalized double-exchange model for magnetic semiconductors with angular momentum j

Randy Fishman^{a,*}, Juana Moreno^b, Mark Jarrell^c

^aCondensed Matter Sciences Division, Oak Ridge National Laboratory, Oak Ridge, TN 37831-6032, USA

^bPhysics Department, University of North Dakota, Grand Forks, ND 58202-7129

^cDepartment of Physics, University of Cincinnati, Cincinnati, OH 45221

Available online 15 November 2005

Abstract

To facilitate the search for new magnetic semiconductors with high transition temperatures T_C , we use dynamical mean-field theory to evaluate T_C for a double-exchange system with general angular momentum $j = 1/2, 3/2, 5/2, \dots$. For simplicity, we assume that there is one local moment per site and that the Hund's coupling J_c between the local moments and the charge carriers (with undoped bandwidth W) is large. The maximum Curie temperature $T_C^{\max}(m_j, j)$ for a given m_j and j occurs when the m_j sub-band is half-filled. For a fixed j , $T_C^{\max}(m_j, j)$ is the largest in the lowest or the highest sub-band with $m_j = \pm j$, where the carriers are most optimally coupled to the local moments. When $j \gg 1$, $T_C^{\max}(\pm j, j)$ scales like $W/\sqrt{2j+1}$, which is the bandwidth of each m_j sub-band. For $j = 1/2$, $T_C^{\max}(\pm 1/2, 1/2)$ is suppressed by fluctuations of the carrier spin. Surprisingly, $T_C^{\max}(\pm j, j)$ reaches a maximum for $j = 3/2$, the same angular momentum as the charge carriers in p -band semiconductors like GaAs and Ge.

© 2005 Elsevier B.V. All rights reserved.

PACS: 75.50.Pp; 02.70.-c; 05.10.-a; 71.27.+a

Keywords: Double exchange; Magnetic semiconductors; Dynamical mean-field theory

The discovery of dilute-magnetic semiconductors (DMS) with angular momentum $j = 3/2$ and transition temperatures above 140 K [1–3] raises an intriguing question: what is the general dependence of T_C on the angular momentum and carrier concentration of a system with exchange coupling between local moments and charge carriers? To answer that question, we use dynamical mean-field theory (DMFT) to calculate the transition temperature of a generalized double-exchange (DE) model. When the Hund's coupling J_c is large enough to break the $(2j+1)$ -degenerate band into well-separated sub-bands, T_C is maximized for $j = 3/2$, which is the angular momentum of the carriers in the well-known semiconductors GaAs and Ge.

Since its development in 1989 by Müller-Hartmann [4] and Metzner and Vollhardt [5], DMFT has become one of

the most powerful many-body techniques for studying electronic models such as the Hubbard [6,7] and DE [8–12] models. Although DMFT becomes exact only in the limit of infinite dimensions, it is believed to accurately capture the physics of correlated electrons even in three dimensions. The utility of DMFT stems from the fact that the self-energy becomes local (i.e. momentum independent) in infinite dimensions [4,5]. Consequently, the local action at site 0 involves a dynamical mean-field $G_0(iv_n)$ associated with the hopping of electrons onto and off site 0, where the electrons experience a local interaction either with each other (as in the Hubbard model) or with an impurity (as in the DE model).

Recent work on DMS materials has used DMFT to study variants of the DE model [13,14] with less than one local moment per site. Since DMFT also becomes exact in the dilute limit, it is a good starting point in the study of DMS systems. A generalized DE model with one local moment per site and large coupling constant J_c provides an upper limit for the transition temperature of a system with

*Corresponding author.

E-mail address: fishmanr@ornl.gov (R. Fishman).

URL: <http://www.ornl.gov/sci/cmsd/theory/fishman.html>.

exchange coupling between the local moments and charge carriers of angular momentum j . There are good reasons to expect that the behavior of $n_h < x$ holes in the impurity band of a DMS with $x < 1$ Mn atoms per site is very similar to that of a DE model with filling $p = n_h/x < 1$ [14]. So long as J_c is sufficiently large to produce a well-defined impurity band, the qualitative results of this model should be independent of the precise magnitude of J_c/W [12]. A generalized DE model with one local moment per site and large J_c also has the distinct advantage that analytical results are possible for any angular momentum j of the charge carriers.

For semiconductors like GaAs, the angular momentum of the holes is given by the vector sum of the $s = 1/2$ spin of the electrons with the $l = 1$ orbital angular momentum of the p bands. The $j = 3/2$ band lies highest in energy while the spin-orbit split $j = 1/2$ band lies about 340 meV below [15]. Consequently, almost all of the holes in Mn-doped GaAs populate the $j = 3/2$ band, which in turn is split by crystal fields [16] into a $m_j = \pm 3/2$ sub-band with heavy holes and a $m_j = \pm 1/2$ sub-band with light holes. These two bands are degenerate at the Γ point with $\mathbf{k} = 0$. More exotic semiconductors with d bands, such as the chalcogenides [17], may contain carriers with total angular momentum $j = 5/2$.

In this paper, we optimize T_C assuming that the band masses of all $2j + 1$ sub-bands are the same. Clearly, this assumption is violated in GaAs where the ratio $r = m_l/m_h$ of the light to heavy band masses is about 0.14. For different band masses, the electronic kinetic energy is diagonalized only when the angular momentum \mathbf{j} is quantized along the momentum \mathbf{k} [16] with $m_j = \mathbf{j} \cdot \mathbf{k}/k$. In related work [14,18], we demonstrate that as r decreases from one, the magnetic frustration introduced by the chirality of the electrons [19] suppresses the maximum T_C for $j = 3/2$. So the calculation presented in this paper provides an upper limit for the transition temperature of a magnetic semiconductor.

The Hamiltonian of a generalized DE model with carriers (holes or electrons) of angular momentum j and equal masses in all sub-bands is given by

$$H = \sum_{\mathbf{k}} \varepsilon_{\mathbf{k}} c_{\mathbf{k}\alpha}^\dagger c_{\mathbf{k}\alpha} - \frac{J_c}{N} \sum_{i,\mathbf{k},\mathbf{k}'} e^{i(\mathbf{k}-\mathbf{k}') \cdot \mathbf{R}_i} \mathbf{S}_i \cdot c_{\mathbf{k}'\alpha}^\dagger \mathbf{J}_{\alpha\beta} c_{\mathbf{k}\beta}, \quad (1)$$

where $c_{\mathbf{k}\alpha}^\dagger$ and $c_{\mathbf{k}\alpha}$ are the creation and destruction operators for an electron with angular-momentum component $m_j = \alpha$ ($\alpha = -j, -j+1, \dots, j$) and momentum \mathbf{k} , $\mathbf{S}_i = \mathbf{S}\mathbf{m}_i$ is the spin of the local moment (treated classically) at site \mathbf{R}_i , and $\mathbf{j}_i = c_{i\alpha}^\dagger \mathbf{J}_{\alpha\beta} c_{i\beta}/2$ is the electronic angular momentum at site i where $\mathbf{J}_{\alpha\beta}$ are the $(2j+1)$ -dimensional angular-momentum matrices (Pauli matrices when $j = 1/2$). Repeated spin indices are summed. Whereas the first term in Eq. (1) represents the electronic kinetic energy, the second term represents the ferromagnetic Hund's coupling between the local-moment spin and the electronic angular momentum. Within DMFT, the local effective

action at any site is given by

$$S_{\text{eff}}(\mathbf{m}) = -T \sum_n \bar{c}_{0\alpha}(iv_n) \{ G_0(iv_n)_{\alpha\beta}^{-1} + \tilde{J}_c \mathbf{J}_{\alpha\beta} \cdot \mathbf{m} \} c_{0\beta}(iv_n), \quad (2)$$

where $\tilde{J}_c = J_c S$, $v_n = (2n+1)\pi T$, $\bar{c}_{0\alpha}(iv_n)$ and $c_{0\alpha}(iv_n)$ are now anticommuting Grassman variables, and $G_0(iv_n)_{\alpha\beta}$ is the dynamical mean-field discussed earlier.

Because $S_{\text{eff}}(\mathbf{m})$ is quadratic in the Grassman variables, the full local Green's function $G(iv_n)_{\alpha\beta}$ may be readily solved by integrating over the Grassman variables, with the result [8] $\underline{G}(iv_n) = \langle \underline{C}^{-1} \rangle_{\mathbf{m}}$, where $\underline{C} = \underline{G}_0(iv_n)^{-1} + \tilde{J}_c \underline{\mathbf{J}} \cdot \mathbf{m}$ is a $(2j+1) \times (2j+1)$ matrix. The average over the orientations \mathbf{m} of the local moment is generally given by $\langle X(\mathbf{m}) \rangle_{\mathbf{m}} = \int d\Omega_{\mathbf{m}} P(\mathbf{m}) X(\mathbf{m})$, where $P(\mathbf{m}) \propto \int_{\bar{c},c} \exp(-S_{\text{eff}}(\mathbf{m}))$ is the probability for the local moment to point in the \mathbf{m} -direction. Above T_C , $P(\mathbf{m}) = 1/4\pi$ is constant. For a semi-circular density of states with full bandwidth W , these relations are closed by the analytic expression [8,7]

$$\underline{G}_0(iv_n)^{-1} = (iv_n + \mu) \underline{I} - \frac{W^2}{16} \underline{G}(iv_n), \quad (3)$$

where μ is the chemical potential corresponding to filling p ($p = 1$ means one electron per site so that $0 \leq p \leq 2j+1$).

Above T_C , the interacting density of states is independent of the band filling. As \tilde{J}_c increases, the $(2j+1)$ -degenerate band splits into $2j+1$ sub-bands, each labeled by quantum number m_j and centered at energy $-2m_j\tilde{J}_c$. Due to the effect of electronic correlations, the full bandwidth of each sub-band is lowered from W to $W' = W/\sqrt{2j+1}$. For $j = 1/2$, this gives the well-known [8] narrowing of each sub-band by $1/\sqrt{2}$. So prior to taking the limit of large \tilde{J}_c for the m_j sub-band, we must rewrite the chemical potential as $\mu = -2m_j\tilde{J}_c + \delta\mu$ where $|\delta\mu| \leq W'/2$.

Close to the ferromagnetic transition, the bare inverse Green's function may be parametrized as $\underline{G}_0(iv_n)^{-1} = (z_n - 2m_j\tilde{J}_c + R_n) \underline{I} + Q_n \underline{J}_z$ where $z_n = iv_n + \delta\mu$. Starting from Eq. (3) for the full Green's function, we find that R_n and Q_n are formally given by the expressions

$$R_n = -\frac{W^2}{16(2j+1)} \int_{\bar{c},c} \langle \underline{C}^{-1} \rangle_{\mathbf{m}}, \quad (4)$$

$$Q_n = -\frac{3W^2}{64j(2j+1)(j+1)} \int_{\bar{c},c} \langle \underline{J}_z \underline{C}^{-1} \rangle_{\mathbf{m}} \quad (5)$$

which use the summation $\sum_{m_j=-j}^j m_j^2 = j(2j+1)(j+1)/3$.

For large J_c and to linear order in the local-moment order parameter $M = \langle m_z \rangle_{\mathbf{m}}$, these relations can be solved by constructing the unitary matrix $\underline{U}_{\mathbf{m}}$ that diagonalizes $\mathbf{m} \cdot \underline{\mathbf{J}}$ with $\underline{U}_{\mathbf{m}} \mathbf{m} \cdot \underline{\mathbf{J}} \underline{U}_{\mathbf{m}}^{-1} = \underline{J}_z$. If $\mathbf{m} = \mathbf{z}$, then $\underline{U}_{\mathbf{m}} = \underline{I}$. When the chemical potential lies in the m_j sub-band, the results $\langle j, m_j | \underline{U}_{\mathbf{m}} \underline{J}_z \underline{U}_{\mathbf{m}}^{-1} | j, m_j \rangle = 2m_j \mathbf{m} \cdot \mathbf{z} = 2m_j m_z$ and

Det \underline{C}

$$\begin{aligned} &= \text{Det}(\underline{U}_m \underline{C} \underline{U}_m^{-1}) \\ &= (2\tilde{J}_c)^{2j} (-1)^{j+m_j} (j+m_j)! (j-m_j)! \\ &\quad \times (z_n + R_n + 2m_j Q_n m_z) \end{aligned} \quad (6)$$

may be used to obtain the solutions

$$R_n = -\frac{z_n}{2} + \frac{1}{2} \sqrt{z_n^2 - \frac{W'^2}{4}}, \quad (7)$$

$$Q_n = \frac{3m_j M}{2j(j+1)} \frac{R_n}{1 - 16m_j^2 R_n^2 / W'^2 j(j+1)}. \quad (8)$$

After integrating $\exp(-S_{\text{eff}}(\mathbf{m}))$ over the Grassman variables, we find that the probability for the local moment to point along \mathbf{m} is

$$\begin{aligned} P(\mathbf{m}) &\propto \exp\left\{ \sum_n \log\left(1 + \frac{2m_j Q_n m_z}{z_n + R_n}\right) \right\} \\ &\propto \exp(\beta J_{\text{eff}} M m_z) \end{aligned} \quad (9)$$

which defines the effective interaction $J_{\text{eff}}(T)$. Finally, T_C is solved from the implicit condition $T_C = J_{\text{eff}}(T_C)/3$.

As a Matsubara sum, the Curie temperature is given by the condition

$$\sum_n \frac{R_n^2}{R_n^2 - j(j+1)W'^2/16m_j^2} = 1 \quad (10)$$

while the filling p is obtained from

$$\begin{aligned} p &= 2T \sum_n \text{Re} \left\{ \frac{1}{z_n + \sqrt{z_n^2 - W'^2/4}} \right\} \\ &\quad + j - m_j + \frac{1}{2}. \end{aligned} \quad (11)$$

Quite naturally, a system with no partially filled sub-band (p an integer) has a vanishing Curie temperature because the carriers are unable to hop to neighboring sites without incurring an infinite cost in coupling energy.

We emphasize that the above derivation of T_C does not assume any specific representation for the angular-momentum j matrices. Rather, we use only the matrix elements of \underline{J}_z : $\langle j, m_j | \underline{J}_z | j, m_j' \rangle = \delta_{m_j, m_j'} 2m_j$.

For finite \tilde{J}_c/W , there are also antiferromagnetic solutions near integer fillings. These solutions arise because when the local moments are ferromagnetically aligned, carriers with the same angular momentum are forbidden to hop between neighboring sites due to the Pauli exclusion principle; but when the local moments are antiferromagnetically aligned, carriers with opposite angular momentum can hop to neighboring sites and back, thereby gaining kinetic energy. For large \tilde{J}_c/W , however, T_N scales like W^2/\tilde{J}_c so that $T_N/W \rightarrow 0$ as $\tilde{J}_c/W \rightarrow \infty$.

For $j = 1/2$ and $3/2$, the dependence of T_C on filling p is plotted in Fig. 1. As expected, T_C is particle-hole symmetric and is the same for systems with p electrons ($2j+1-p$ holes) or p holes ($2j+1-p$ electrons) per site.

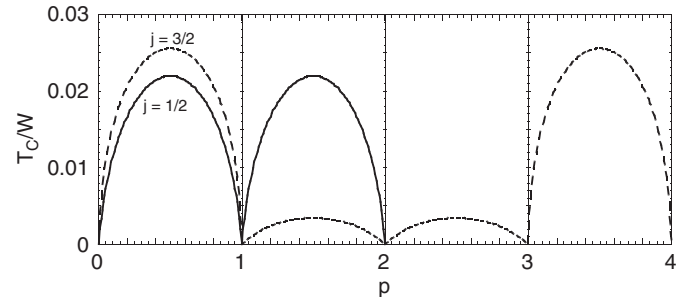


Fig. 1. The dependence of T_C/W on filling p for $j = 1/2$ (solid) and $3/2$ (dashed). For $j = 1/2$, $0 \leq p \leq 2$ while for $j = 3/2$, $0 \leq p \leq 4$.

Notice that T_C is also particle-hole symmetric within each sub-band. Hence, the largest Curie temperature within each sub-band is obtained when that sub-band is half-filled with $\delta\mu = 0$. The highest T_C occurs in the sub-bands with $m_j = \pm j$ because those holes or electrons are able to most effectively take advantage of the exchange coupling that mediates the ferromagnetism between the local moments. Remarkably, the maximum T_C for $j = 3/2$ in the $m_j = \pm 1/2$ sub-bands is only about 14% of the maximum T_C in the $m_j = \pm 3/2$ sub-bands. Compared to the maximum T_C for $j = 1/2$ of $0.0219W$, the maximum T_C for $j = 3/2$ of $0.0256W$ is about 16% higher.

For a half-filled sub-band, we obtain an analytic expression for T_C by converting the Matsubara sum into an integral (assuming that T_C/W is small), with the result

$$\begin{aligned} \frac{T_C^{\text{max}}(m_j, j)}{W} &\approx \frac{1}{4\pi\sqrt{2j+1}} \left\{ 1 - \frac{j(j+1) - m_j^2}{2m_j\sqrt{j(j+1)}} \right. \\ &\quad \left. \times \tan^{-1} \left(\frac{2m_j\sqrt{j(j+1)}}{j(j+1) - m_j^2} \right) \right\}. \end{aligned} \quad (12)$$

This expression yields values for the Curie temperature that are only slightly larger than the exact result, Eq. (10). The maximum T_C for $m_j = \pm j$ is then given approximately by

$$\begin{aligned} \frac{T_C^{\text{max}}(\pm j, j)}{W} &\approx \frac{1}{4\pi\sqrt{2j+1}} \left\{ 1 - \frac{1}{2\sqrt{j(j+1)}} \right. \\ &\quad \left. \times \tan^{-1} \left(2\sqrt{j(j+1)} \right) \right\}, \end{aligned} \quad (13)$$

which is plotted versus angular momentum j in Fig. 2. For large j , $T_C^{\text{max}}(\pm j, j)/W' \rightarrow (1/4\pi)\{1 - \pi/4j\}$ saturates at $1/4\pi$. Of course, only half-integer j 's are allowed.

To interpret Fig. 2, keep in mind that in the absence of magnetic impurities, a semiconductor is characterized by the bandwidth W of the conduction band and by the angular momentum j of the charge carriers. After doping with magnetic impurities, the bandwidth W' of the impurity band will be narrowed by electronic correlations compared with the bandwidth W of the parent compound. So for a class of undoped materials with the same bandwidth W , the transition temperature is maximized

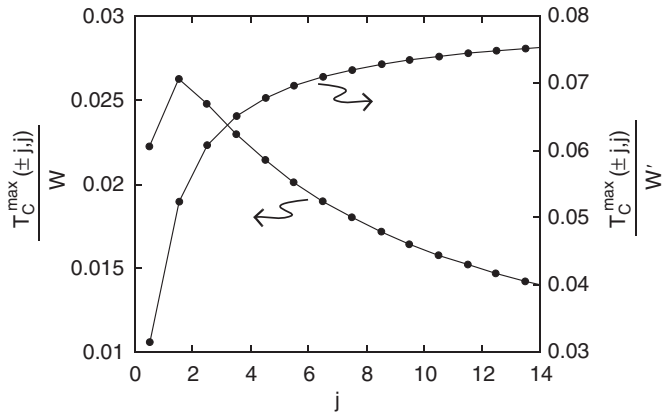


Fig. 2. The transition temperature $T_C^{\max}(\pm j, j)$ (in the lowest or highest sub-band) versus j normalized by either W or W' .

when $j = 3/2$. On the other hand, for a class of doped materials with the same impurity bandwidth W' , the transition temperature is a monotonically increasing function of j that saturates at the value $W'/4\pi$.

Judging by these results alone, it would seem unlikely that more exotic semiconductors with $j > 3/2$ will have higher transition temperatures than Mn-doped GaAs or Ge. But in separate work [14,18], we show that suppression of T_C due to magnetic frustration may be quite a bit larger than the small difference between the optimized Curie temperatures for $j = 3/2$ and $5/2$ in Fig. 2. So a magnetic semiconductor with $j = 5/2$ and nearly equal band masses may easily have a higher transition temperature than one with $j = 3/2$ and a small value of the ratio of masses, m_l/m_h .

A serious but unavoidable weakness of the present approach is that the spins of the local moments and charge carriers are not treated on the same footing: whereas the local moments are treated classically, the charge carriers are not. When the spin S of the local moment is much larger than the angular momentum j of the charge carriers, this approximation should be a very good one. But when S becomes comparable to j , fluctuations of the local-moment spin may further suppress the transition temperature due to the exchange coupling with the charge carriers. Thus, the optimum magnetic semiconductor has $j = 3/2$, equal band masses, and $S \gg j$. The last condition is not satisfied in Mn-doped GaAs, where $j = 3/2$ and $S = 5/2$ [3].

This paper has examined the general dependence of the transition temperature of a magnetic semiconductor on the angular momentum and filling of the charge carriers. For a

fixed bandwidth of the parent compound, T_C is maximized when $j = 3/2$, the same angular momentum carried by the charge carriers in GaAs and Ge. Our work suggests that the best way to optimize the transition temperature of magnetic semiconductors may be to minimize the effects of magnetic frustration in $j = 3/2$ materials.

Acknowledgements

We gratefully acknowledge useful conversations with Horacio Castillo and Igor Žutić. This research was sponsored by the U.S. Department of Energy under contract DE-AC05-00OR22725 with Oak Ridge National Laboratory, managed by UT-Battelle, LLC and by the National Science Foundation under Grant Nos. DMR-0312680 and EPS-0132289 (ND EPSCOR).

References

- [1] H. Ohno, A. Shen, F. Matsukura, A. Oiwa, A. Endo, S. Katsumoto, Y. Iye, Appl. Phys. Lett. 69 (1996) 363.
- [2] H. Munekata, H. Ohno, S. von Molnár, Armin Segmüller, L.L. Chang, L. Esaki, Phys. Rev. Lett. 63 (1989) 1849.
- [3] For a recent review, see A.H. MacDonald, P. Schiffer, N. Samarth, Nat. Mat. 4 (2005) 195.
- [4] E. Müller-Hartmann, Z. Phys. B 74 (1989) 507; E. Müller-Hartmann, Z. Phys. B 76 (1989) 211.
- [5] W. Metzner, D. Vollhardt, Phys. Rev. Lett. 62 (1989) 324.
- [6] J.K. Freericks, M. Jarrell, Phys. Rev. Lett. 74 (1995) 186.
- [7] Applications of DMFT to the Hubbard model and additional references are contained in the comprehensive review article: A. Georges, G. Kotliar, W. Krauth, M.J. Rozenberg, Rev. Mod. Phys. 68 (1996) 13.
- [8] N. Furukawa, J. Phys. Soc. Jpn. 64 (1995) 2754; N. Furukawa, J. Phys. Soc. Jpn. 64 (1995) 3164.
- [9] A.J. Millis, R. Mueller, B.I. Shraiman, Phys. Rev. B 54 (1996) 5389; A.J. Millis, R. Mueller, B.I. Shraiman, Phys. Rev. B 54 (1996) 5405; B. Michaelis, A.J. Millis, Phys. Rev. B 68 (2003) 115111.
- [10] M. Auslender, E. Kogan, Phys. Rev. B 65 (2001) 012408; M. Auslender, E. Kogan, Europhys. Lett. 59 (2002) 277.
- [11] R.S. Fishman, M. Jarrell, J. Appl. Phys. 93 (2003) 7148; R.S. Fishman, M. Jarrell, Phys. Rev. B 67 (2003) 100403.
- [12] A. Chernyshev, R.S. Fishman, Phys. Rev. Lett. 90 (2003) 177202.
- [13] A. Chattopadhyay, S. Das Sarma, A.J. Millis, Phys. Rev. Lett. 87 (2001) 227202.
- [14] K. Aryanpour, J. Moreno, M. Jarrell, R.S. Fishman, Phys. Rev. B 72 (2005) 045343.
- [15] J.S. Blakemore, J. Appl. Phys. 53 (1982) R123.
- [16] J.M. Luttinger, W. Kohn, Phys. Rev. 97 (1955) 869.
- [17] A. Mauger, C. Godart, Phys. Rep. 141 (1986) 51 and reference therein.
- [18] J. Moreno, R.S. Fishman, M. Jarrell, unpublished.
- [19] G. Zaránd, B. Jankó, Phys. Rev. Lett. 89 (2002) 047201.